CORPUS PUBLISHERS

Journal of Mineral and Material Science (JMMS)

ISSN: 2833-3616

Volume 6 Issue 2, 2025

Article Information

Received date : February 10, 2025

Published date: February 25, 2025

*Corresponding author

Zheng Yin, Key Laboratory of Auxiliary Chemistry and Technology for Chemical Industry, Ministry of Education, Shaanxi Collaborative Innovation Center of Industrial Auxiliary Chemistry and Technology, College of Chemistry and Chemical Engineering, Shaanxi University of Science and Technology, Xi'an 710021, P. R. China,

Xi'an Lanqiao New Energy Technology Co., LTD, Xi'an 710018.

DOI: 10.54026/JMMS/1109

Key Words

Microstructures; Electrodes; Vanadium Redox Battery; Carbon Emission

Short Communication

ZIF-67 Derived Porous Carbon Microstructures Modified Electrodes for High-performance Vanadium Redox Flow Batteries

Ke-Ke Jiang[1], Dan-Jiang Tang[1,2], Peng-Wei Zhang[2*], Ge Huo[3], and Zheng Yin[1,2*]

[1]*Key Laboratory of Auxiliary Chemistry and Technology for Chemical Industry, Ministry of Education, Shaanxi Collaborative Innovation Center of Industrial Auxiliary Chemistry and Technology, College of Chemistry and Chemical Engineering, Shaanxi University of Science and Technology, Xi'an 710021, P. R. China*

[2]*Xi'an Lanqiao New Energy Technology Co., LTD, Xi'an 710018, P. R. China*

[3]*Shaanxi Engineering Research Center of Controllable Neutron Source, College of Electronics and Information Engineering, Xijing University, Xi'an, 710123, People's Republic of China*

Abstract

Graphite felts (GF) has been used as electrode material for VRFBs, yet surface modification is necessary to improve electrochemical activity and hydrophilia. Herein, a porous carbon modified electrode ZIF-67-GF@450-A was prepared by a ZIF-67 combination, calcination at 450 °C and subsequent acid etching. It was shown that the uniformly distributed carbon microstructures introduced to the microfilaments of graphite felt enhanced the electrodes performance, and promoted VO^{2+}/VO_2^+ redox reaction. As a result, the all-vanadium redox flow battery (VRFB) assembled with ZIF-67-GF@450-A as the electrode could maintain energy efficiency (EE) of 82.09% and 71.33% at current densities of 200 mA cm^{-2} and 400 mA cm^{-2}, respectively, with a discharge capacity of 477.5 mAh at 400 mA cm^{-2}. This electrode modification method provides valuable insights for the further improvement of high-performance VRFB.

Introduction

It is imperative to accelerate the development of green and renewable energy to reach zero carbon emission. Representative renewable energy sources like wind and solar power is fluctuating and susceptible to several environmental parameters [1]. To address these challenges, the development of large-scale energy storage system is indispensable to construct the energy cycle. The all-vanadium redox flow battery (VRFB) stands out as an ideal solution due to its high energy efficiency, enough safety and long service life [2]. Nevertheless, enhancing power density remains a critical objective to further improve economic viability of VRFB. In various research directions, an increasing number of researchers are focusing on improving the electrochemical performance of electrodes. The power density of a VRFB system is fundamentally determined by the rate of the redox reactions occurring at the electrode-electrolyte interface. The microstructure and surface characteristics of the electrode play a critical role to determine the reaction rate. By improving the electrochemical performance of the electrodes, it is possible to significantly boost the power density of VRFB systems [3]. Therefore, it is imperative to develop new electrode materials with high catalytic activity and large specific surface areas.

In recent years, the most commonly used electrode materials in VRFBs are graphite felt, carbon felt, and carbon paper, which are three-dimensional porous carbon materials that are chemically stable and cost-effective [4]. However, their poor hydrophilicity and limited specific surface areas lead to insufficient electrochemical activity. These materials can only be used at low current densities in VRFBs. On this occasion, modifications to electrode materials are necessary, which includes surface treatments of heat treatment [5], acid treatment [6], microwave treatment [7], and heteroatom doping (e.g., N, P, F) [8], as well as catalyst introduction of metal catalysts[9~12], carbon-based catalysts[13], and metal-carbon composite catalysts [14].

In recent years, metal-organic frameworks (MOFs) and their datives have garnered significant interest within the electrochemical domain. MOFs are not only capable of acting as electrocatalysts independently but can also be readily converted into metal oxides or porous carbons under uncomplicated conditions [15]. In this paper, cobalt based ZIF-67 was selected as the precursor, which was firmly bonded with graphite mats by the as-grown method. Then, the carbon microstructures modified electrode was obtained step-by-step through ZIF-67 combination, calcination at 450 °C and subsequent acid etching. The microfilaments of graphite felt uniformly and firmly decorated with abundant carbon nanoparticles, which not only provided a large number of reactive sites but also increased the accessibility to the electrolyte. Thereby, the migration rate of the electrolyte on the electrode surface improved and the overall performance of VRFB enhanced. The presented post-treatment modification provides a reference for preparing high-performance electrodes and promotes the advance of VRFB.

Preparation of modified electrodes and battery

The pristine GF was heated at 400 °C for 8 hours in an air atmosphere, and the generated produce was named as TGF. The electrode was fabricated utilizing a static MOFs growth technique, followed by thermal calcination and acidic etching. Initially, 1 mmol $Co(NO_3)_2\cdot6H_2O$ and 4 mmol 2-methylimidazole were dissolved in 25 mL methanol, respectively, and the purple solution was formed after the mixture of the two. Subsequently, a piece of TGF sized at 3.0 cm × 3.0 cm with thickness of 4 mm was submersed into the purple solution, allowing for a static growth period of 24 hours at ambient temperature. Uniform growth of ZIF-67 particles on the GF fibers were obtained. Then the GF were dried at a temperature of 60 °C for a duration of 12 hours, yielding the ZIF-67@GF sample. This ZIF-76 containing GF was subsequently placed within a tubular furnace, where it was heated to a temperature of 450 °C for 2 hours under a nitrogen atmosphere. The samples underwent further etching in an 8 mol L-1 sulfuric acid solution for 24 hours, followed by washing to pH neutrality with deionized water and drying in an oven at 80 °C. The resultant product was designated as ZIF-67-GF@450-A. The all-vanadium liquid flow single cell was provided by Wuhan Zhisheng Co, using modified graphite felts as the positive and negative electrodes, and Nafion 212 was used as the ion-exchange membrane.

Morphological and structural characterization

The surface morphology of TGF and ZIF-67-GF@450-A was examined using SEM (Figure 1). The TGF exhibited a very smooth surface with distinct texturing. In contrast, after carbonization and acid treatment, the surface of ZIF-67-GF@450-A displayed a significant presence of carbon nanoparticles. The EDX analysis of AE-GF revealed uniform distribution of C and O elements on the carbon fiber surface, while no Co element was detected, indicating that the acid treatment effectively removed cobalt oxides. This uniform dispersion of carbon nanoparticles significantly enhanced the active sites on the electrode surface, thereby improving the contact with the electrolyte and substantially enhancing the redox reaction kinetics.

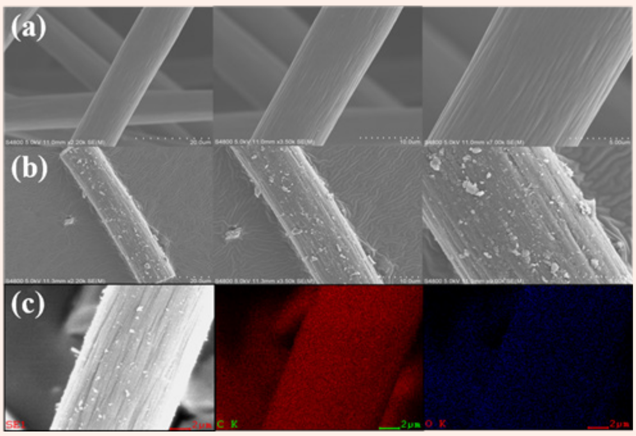

Figure 1: SEM images of (a) TGF, (b) ZIF-67-GF@450-A, (c) EDX elemental mapping images of ZIF-67-GF@450-A.

Powder X-ray diffraction (PXRD) analyses, featuring well-matched experimental and simulated spectra, confirmed the high crystallinity and purity of the synthesized ZIF-67 (Figure 2(a)). Figure 2(b) illustrates the PXRD patterns of TGF and ZIF-67-GF@450-A, both exhibiting broad peaks at 25.3° and 43.2°, corresponding to the (002) and (100) crystal planes of graphite materials, respectively. Notably, the absence of Co_3O_4 diffraction peaks in ZIF-67-GF@450-A confirms the complete removal of cobalt oxides. Raman spectroscopy was utilized to evaluate structural defects and the degree of graphitization in the samples. All carbon materials exhibited distinct characteristic peaks at 1350 cm^{-1} (D band) and 1590 cm^{-1} (G band) (Figure 2(c)). The I_D/I_G ratios for TGF and ZIF-67-GF@450-A were measured as 1.51 and 1.20, respectively, indicating a more ordered crystalline structure for ZIF-67-GF@450-A. Figure 2(d) presents a comparison of the water contact angle measurements for TGF and ZIF-67-GF@450-A, with respective contact angles of 110.6° and 0°. These results demonstrate that the wettability of ZIF-67-GF@450-A was markedly enhanced after calcination and acidic treatment, thereby significantly reducing the contact resistance between the electrolyte and the electrode.

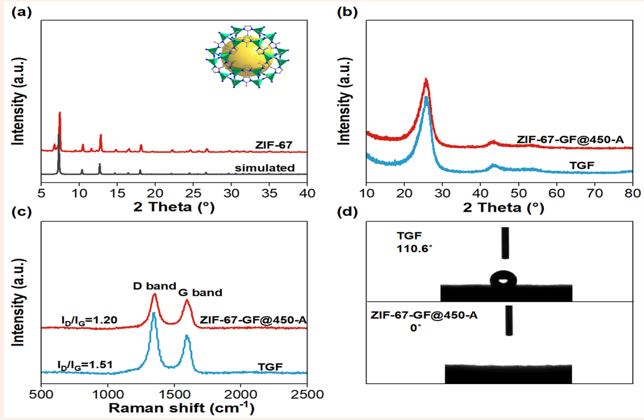

Figure 2: The PXRD pattern for (a) ZIF-67 and (b) TGF and ZIF-67-GF@450-A. The comparison of (c) Raman spectrum and (d) water contact angle test for TGF and ZIF-67-GF@450-A.

Electrochemical measurements

The CV and EIS tests of the positive electrode were conducted in a 0.1 mol L^{-1} + 3.0 mol L^{-1} H_2SO_4 solution. Figure 3(a) illustrates the CV curves of ZIF-67-GF@450-A at scan rates ranging from 1 to 20 mV s^{-1}. The results demonstrate well-defined and symmetrical oxidation and reduction peaks across all scan rates, indicating that ZIF-67-GF@450-A exhibits a pronounced electrocatalytic effect on the VO^{2+}/VO^{2+} redox reaction. Specifically, at a scan rate of 5 mV s^{-1}, the onset potentials for both oxidation and reduction of ZIF-67-GF@450-A are higher compared to those of TGF, as shown in Figure 3(b). This indicates that the VO^{2+}/VO_2^+ redox reaction occurs more readily on ZIF-67-GF@450-A, which exhibits superior electrochemical reaction activity. Similarly, the peak potential separation for ZIF-67-GF@450-A decreases from 380 mV to 280 mV for TGF. Additionally, the ratio of the oxidation and reduction peak currents ($-I_{pc}/I_{pa}$) for ZIF-67-GF@450-A is closer to 1. These findings suggest that the electrochemical reversibility of ZIF-67-GF@450-A is significantly better than that of TGF. Figure 3(c) illustrates the relationship between the peak current density and the square root of the scan rate for TGF and ZIF-67-GF@450-A across the entire scan rate range. Both materials exhibit a linear relationship; however, the slope for ZIF-67-GF@450-A is higher. The redox reactions of vanadium ions are predominantly influenced by mass diffusion at both the positive and negative electrodes. Consequently, ZIF-67-GF@450-A demonstrates a higher mass transfer rate and electrochemical reaction area. Figure 3(d) illustrates the EIS analysis of the VO^{2+}/VO_2^+ redox reaction at a potential of 0.8 V, aimed at evaluating the charge transfer capability at the electrode-electrolyte interface. The ZIF-67-GF@450-A electrode exhibits the smallest semicircle diameter at high frequencies, indicating that the abundance of redox-active sites on this electrode leads to the lowest charge transfer resistance. This finding aligns with the CV curve results, further corroborating the enhanced electrochemical performance of the ZIF-67-GF@450-A electrode.

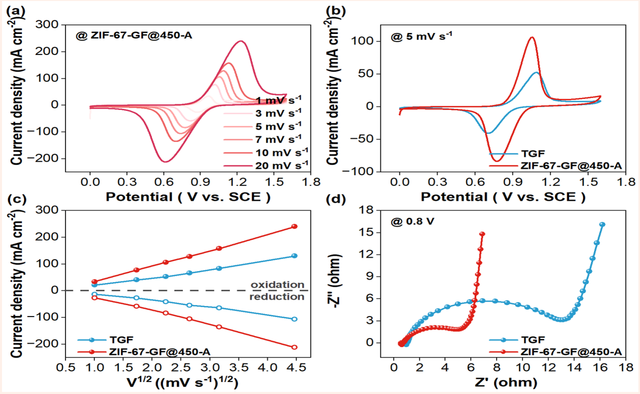

Figure 3: (a) CV test curves of ZIF-67-GF@450-A at sweep rates ranging from 1 to 20 mV s^{-1}. (b) CV test curves at 5 mV s^{-1} in the cathode electrolyte. (c) Plot of peak redox current density versus the square root of the sweep rate in the cathode electrolyte. (d) EIS spectra in the cathode electrolyte.

VRFB single cell performance

The ZIF-67-GF@450-A electrode was utilized to assemble a single vanadium redox flow battery (VRFB) cell to investigate the impact of the modified electrode on battery performance. For comparison, a TGF electrode was employed in an unmodified control cell. Figure 4(a) shows the discharge capacities of both cells at current densities ranging from 80 to 400 mA cm^{-2}. The data clearly indicate that as the current density increases, the discharge capacity decreases for both cells. However, the modified cell consistently exhibits higher discharge capacity compared to the control cell across all tested current densities. Notably, the modified cell maintains operation at a maximum working current density of 400 mA cm^{-2}, whereas the control cell ceases functioning at this density due to significant battery polarization. Specifically, at a current density of 360 mA cm^{-2}, the modified cell exhibits a discharge capacity of 515.6 mAh, compared to only 187.3 mAh for the control cell. Furthermore, at 400 mA cm^{-2}, the modified cell sustains a discharge capacity of 477.5 mAh, as illustrated in Figures 4(b) and 4(c). The graphs in Figure 4(d) illustrate the Coulombic efficiency (CE) and voltage efficiency (VE) of the respective cells. CE primarily measures the charge loss associated with ionic transport across the membrane. Since both cells employ the same Nafion membrane and electrolyte, their CE values at corresponding current densities are nearly identical. VE, which primarily assesses the degree of battery polarization, is significantly higher for the modified cell across all current densities, indicating that the ZIF-67-GF@450-A electrode can enhance battery performance by reducing polarization effects. Energy efficiency (EE), a composite metric for evaluating battery performance, is the product of Coulombic efficiency (CE) and voltage efficiency (VE). Consequently, it reflects the trend of VE, as illustrated in Figure 4(e). At a current density of 200 mA cm^{-2}, the modified cell achieves a VE of 85.85% and EE of 82.09%, respectively, representing improvements of 7.92% and 8.82% over the control cell. At 400 mA cm^{-2}, the modified cell sustains a VE of 74.05% and an EE of 71.33%. Figure 4(f) illustrates the average charge and discharge voltages for both cells at different current densities. Compared to the control cell, the modified cell exhibits lower charging voltage and higher discharging voltage, highlighting its superior electrochemical performance, reduced battery polarization, and enhanced overall battery efficiency.

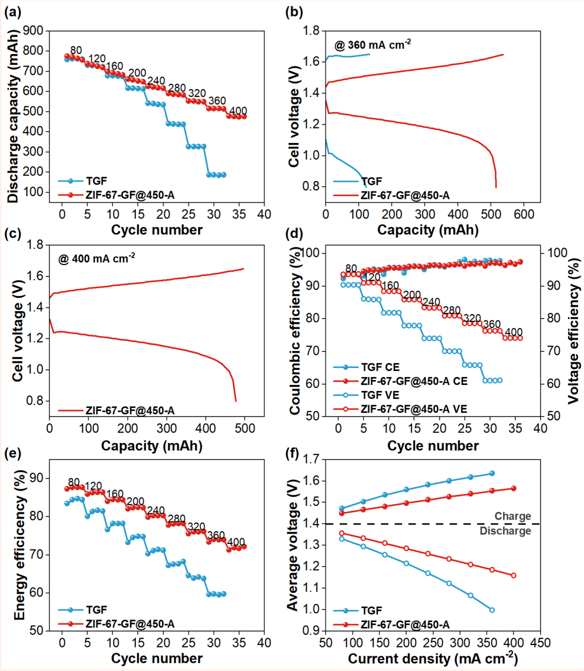

Figure 4: Pristine and modified cells: (a) discharge capacity at various current densities, (b) charge-discharge curves at 360 mA cm^{-2}, (c) charge-discharge curves at 400 mA cm^{-2}, (d) CE and VE, (e) EE, (f) average voltage during charging and discharging.

In summary, this study successfully prepared ZIF-67-derived porous carbon microstructures modified graphene fiber electrodes using a straightforward in-situ ZIFs growth technique, followed by thermal calcination and acid treatment. The surface modification of the electrodes with porous carbon microstructures not only enhanced the availability of active sites for the VO^{2+}/VO_2^+ redox couple but also facilitated ionic migration within the electrolyte. As a result, the VRFBs employing these modified electrodes as cathodes and anodes exhibited an energy efficiency of 82.09% at a current density of 200 mA cm^{-2}. Even at a higher current density of 400 mA cm^{-2}, the energy efficiency remained at 71.33%, accompanied by a high discharge capacity of 477.5 mAh. The improved electrochemical performance of the modified electrodes and VRFBs can be attributed to the increased electrode hydrophilicity and the introduction of additional defects on the carbon fiber surface. Given the vast library of MOFs and their derived nanocomposites, these findings pave the way for extensive electrode modifications to enhance VRFB properties.

Acknowledgment

This work was supported by the National Natural Science Foundation of China (No. 22371173), Scientific Research Project of Education Department of Shaanxi Province (No. 22JC014), and the Qinchuangyuan Scientist & Engineer Project of Shaanxi Province (No. 2024QCY-KXJ-135).

References

1. Marcel CP (2023) Addressing the global energy problem: Perspectives, challenges, and potential solutions. Nucl Eng Des 414: 112610.
2. Trovò A, Rugna M, Poli N, Guarnieri M (2023) Prospects for industrial vanadium flow batteries. Ceram Int 49(14): 24487-24498.
3. Xu J, Zhang Y, Huang Z, Jia C, Wang S (2021) Surface Modification of Carbon-Based Electrodes for Vanadium Redox Flow Batteries. Energ Fuel 35(10): 8617-8633.
4. Hossain MH, Abdullah N, Tan KH, Saidur R, Radzi MAM, et al. (2024) Evolution of Vanadium Redox Flow Battery in Electrode. Chem Rec 24(1): e202300092.
5. Greco KV, Forner-Cuenca A, Mularczyk A, Eller J, Brushett FR (2018) Elucidating the Nuanced Effects of Thermal Pretreatment on Carbon Paper Electrodes for Vanadium Redox Flow Batteries. ACS Appl Mater 10(51): 44430-44442.
6. Hassan A, Tzedakis T (2019) Enhancement of the electrochemical activity of a commercial graphite felt for vanadium redox flow battery (VRFB), by chemical treatment with acidic solution of $K_2Cr_2O_7$. J Energy Storage 26: 100967.
7. Wu X, Xu H, Xu P, Shen Y, Lu L, et al. (2014) Microwave-treated graphite felt as the positive electrode for all-vanadium redox flow battery. J. Power Sources 263: 104-109.
8. Su Y, Chen N, Ren HI, Li CW, Li Z, et al. (2023) Application of modified graphite felt as electrode material: a review. Carbon Lett 33(1): 1-16.
9. Mehboob S, Ali G, Shin HJ, Hwang J, Abbas S, et al. (2018) Enhancing the performance of all-vanadium redox flow batteries by decorating carbon felt electrodes with SnO_2 nanoparticles. Appl Energy 229: 910-921.
10. Kabtamu DM, Chang YC, Lin GY, Bayeh AW, Chen JY (2017) Three-dimensional annealed WO3 nanowire/graphene foam as an electrocatalytic material for all vanadium redox flow batteries. Sustain. Energ Fuels 1(10): 2091-2100.
11. Vázquez-Galván J, Flox C, Jervis JR, Jorge AB, Shearing PR, et al. (2019) High-power nitrided TiO2 carbon felt as the negative electrode for all-vanadium redox flow batteries. Carbon 148: 91-104.
12. Zhou H, Shen Y, Xi J, Qiu X, Chen L (2016) ZrO_2-Nanoparticle-Modified Graphite Felt: Bifunctional Effects on Vanadium Flow Batteries. ACS Appl Mater 8(24): 15369-15378.
13. Deng Q, Huang P, Zhou WX, Ma Q, Zhou N, et al. (2017) A High-Performance Composite Electrode for Vanadium Redox Flow Batteries. Adv Energy Mater 7(18): 1700461.
14. He Z, Dai L, Liu S, Wang L, Li C (2015) Mn_3O_4 anchored on carbon nanotubes as an electrode reaction catalyst of V(IV)/V(V) couple for vanadium redox flow batteries. Electrochim Acta 176: 1434-1440.
15. Li Y, Ma L, Yi Z, Zhao Y, Mao J, et al. (2021) Metal-organic framework-derived carbon as a positive electrode for high-performance vanadium redox flow batteries. J Mater Chem A 9(9): 5648-5656.